Galaxy^3-lensing in the CFHTLenS: preliminary results

Patrick Simon[†] & Thomas Erben[†],

Henk Hoekstra, Catherine Heymans, Hendrik Hildebrandt, Thomas Kitching, Yannick Mellier, Lance Miller, Ludovic Van Waerbeke, Jean Coupon, Liping Fu, Mike Hudson, Konrad Kuijken, Barney Rowe, Tim Schrabback, Elisabetta Semboloni, Malin Velander

[†]AIfA, Universität Bonn, Auf dem Hügel 71, 53121, Germany

Argelander-Institut für Astronomie

Lens and source samples

Only galaxies from the CFHTLenS object catalogue with photo-z estimates (`BPz`; bands $ugriz$) and $m_{\rm R} \le 24.5\,{\rm mag}$ are considered as potential lenses or sources. The survey has 146 patches with $1\,{\rm deg}^2$ each; $M_{\rm r}$ and $M_{\rm u}$ are SDSS filters.

- **Lenses** are selected to represent red galaxies with restframe $M_{\rm u} - M_{\rm r} \in [1.5, 3.0]\,{\rm mag}$ from a photo-z interval $z \in [0.15, 0.6]$ ($\bar{z} \approx 0.4$). For the analysis, the lens sample is further sub-divided into $M_{\rm r}$-bins out of $[-25, -16]\,{\rm mag}$. The lens number density is roughly $1.5\,{\rm arcmin}^{-2}$ for the total sample.
- **Sources** have $z \in [0.7, 1.2]$ so that there should be little z-overlap between the lens and source sample, let alone for a few extreme outliers. The effective number density of sources (weighed in analysis) is $\sim 3\,{\rm arcmin}^{-2}$ with $\bar{z} \approx 0.9$. Source ellipticities are estimated by `LENSFIT`.

Conclusions

- We present a successful measurement of G3L in the CFHTLenS (red lenses at $\bar{z} \approx 0.4$) and, for the first time, a highly significant measurement of the shear-shear-lens correlation function (Fig. 1 and Fig. 2; Table 2).
- Systematics indicators of G3L are consistent with zero in almost all lens magnitude bins (Table 2).
- There is, observed for the first time, for smaller scales ($\theta_{\rm ap} \lesssim 5'$) a change in the lens-lens-shear correlation with $M_{\rm r}$-luminosity but, so far, no detectable change in the shear-shear-lens correlation (Table 1).
- The results are, on a order-of-magnitude level, comparable to earlier measurements in the RCS [2], albeit a bit higher as we focus on red lenses here.

Results: luminosity dependence

The aim here is to test the null hypothesis that the same type of G3L correlation function are equal for distinct lens magnitudes. With a Gaussian noise model as assumption, the χ^2 of difference signals is computed. The noise covariance of the difference signal is the sum of the individual magnitude bin covariances as estimated from the field-to-field variance. We find some $M_{\rm r}$-dependence in $\langle \mathcal{N}^2 M_{\rm ap} \rangle$.

	[-17,-16]	[-18,-17]	[-19,-18]	[-20,-19]	[-21,-20]	[-22,-21]	[-25,-22]
[-17,-16]	.	60.5%	7.7%	18.5%	8.1%	3.7%	5.5%
[-18,-17]	91.6%	.	53.4%	71.3%	7.4%	0.6%	0.5%
[-19,-18]	95.5%	99.9%	.	49.8%	0.2%	0.2%	0.2%
[-20,-19]	80.8%	99.9%	90.9%	.	78.3%	29.5%	28.9%
[-21,-20]	57.4%	98.7%	76.3%	97.1%	.	36.2%	20.1%
[-22,-21]	47.2%	73.5%	50.8%	95.4%	68.1%	.	62.1%
[-25,-22]	63.7%	66.3%	53.2%	63.2%	62.2%	62.4%	.

Table 1: Percentage p-values of a χ^2 assuming equal signals in distinct lens magnitude bins. Red values reject the null hypothesis with 5% error. Blue: $\langle \mathcal{N}^2 M_{\rm ap} \rangle$, orange: $\langle \mathcal{N} M_{\rm ap}^2 \rangle$.

Results: signal and possible systematics

To assess the significance of the results (Fig. 1 and Fig. 2), we test the null hypothesis that the measurement is consistent with a zero assuming Gaussian noise statistics; the χ^2 relative to zero is computed. The covariance for the noise model is determined from the field-to-field variance between all CFHTLenS patches. Table 2 shows the p-values of this test for the E-mode but also for the B- and P-modes, both serving as systematics indicators. Almost throughout E-modes are significantly non-zero, B-modes are zero.

	E-mode	B-mode	E-mode	B-mode	P-mode
[-17,-16]	0.00%	50.5%	5.0%	28.9%	93.2%
[-18,-17]	0.00%	56.4%	2.0%	39.0%	14.2%
[-19,-18]	0.00%	2.0%	0.1%	95.6%	77.5%
[-20,-19]	0.00%	55.0%	2.8%	63.4%	84.4%
[-21,-20]	0.00%	17.6%	0.1%	43.6%	72.6%
[-22,-21]	0.00%	99.5%	2.2%	96.9%	92.1%
[-25,-22]	0.00%	73.9%	98.7%	52.4%	56.6%

Table 2: Percentage p-values of a χ^2 assuming a zero signal. Red values reject the null hypothesis with 5% error. Blue: $\langle \mathcal{N}^2 M_{\rm ap} \rangle$, orange: $\langle \mathcal{N} M_{\rm ap}^2 \rangle$.

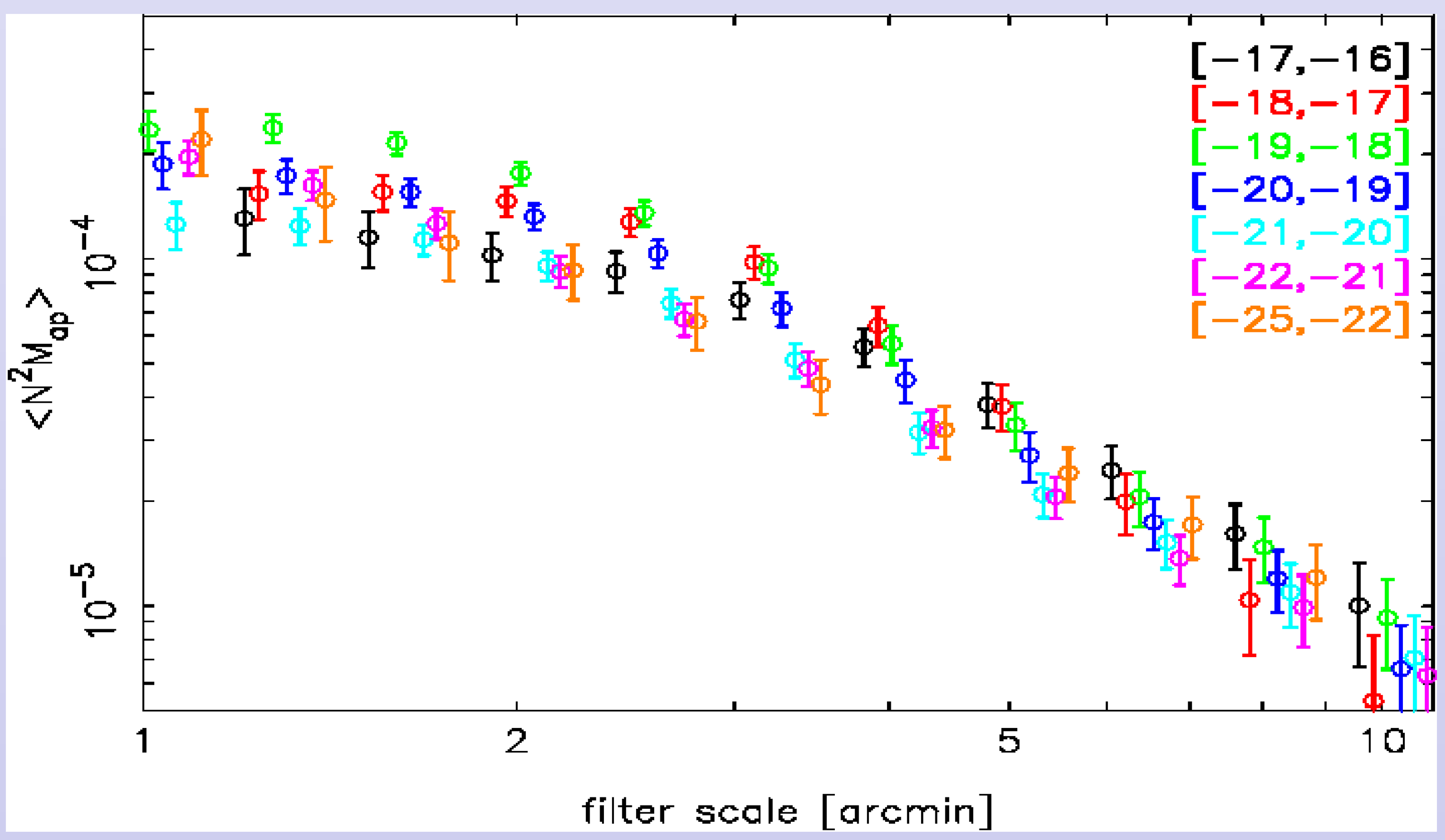

Fig. 1: Lens-lens-shear correlation function disguised as E-mode aperture statistics for different aperture filter scales and different lens $M_{\rm r}$-bins. Error bars are standard deviations of the mean from all fields.

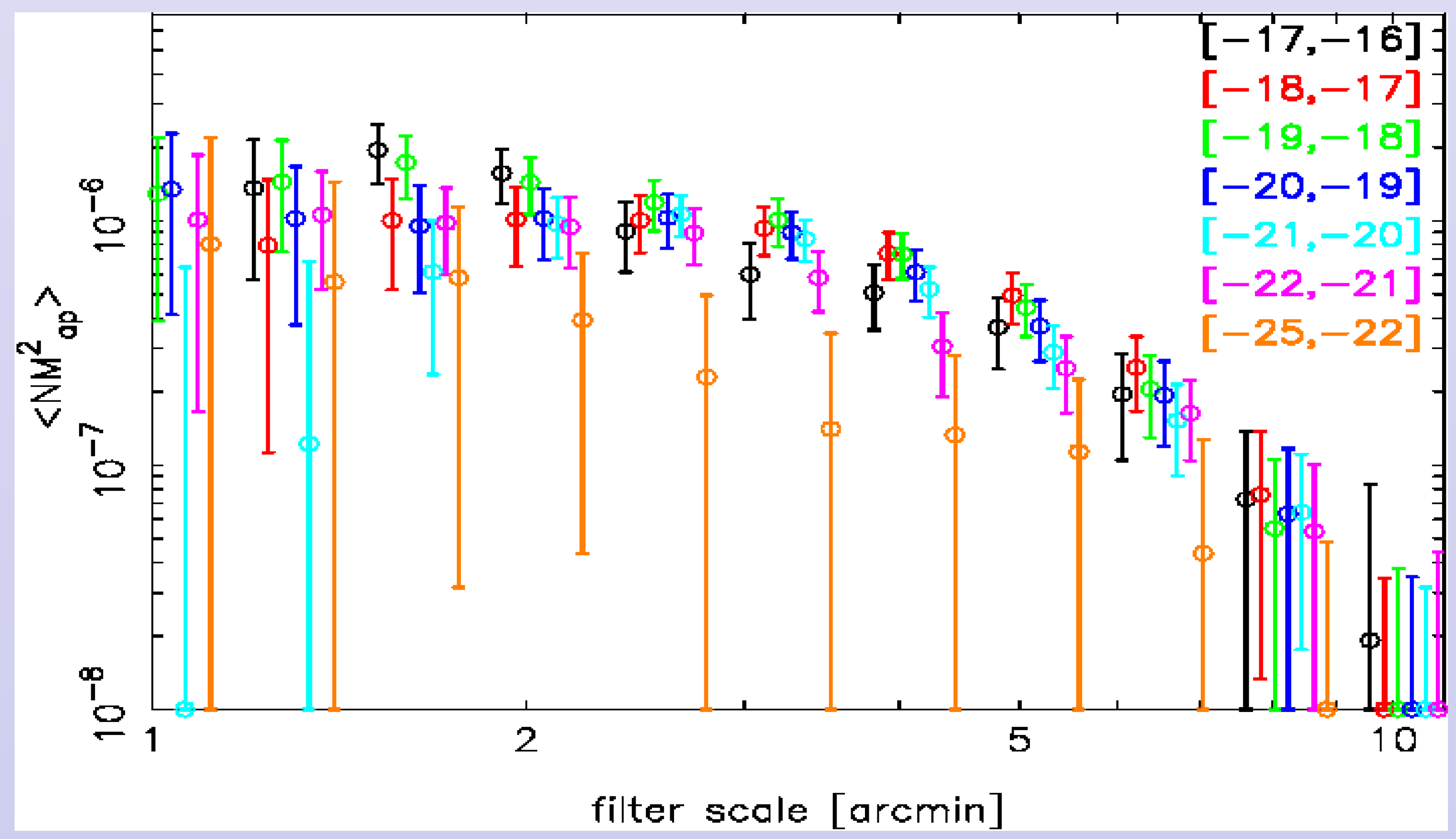

Fig. 2: Same as Fig. 1 but here for the E-mode of the shear-shear-lens correlation function. Contrary to Fig. 1, no signal change with $M_{\rm r}$ is detected.

Third-order galaxy-galaxy lensing in a peanutshell

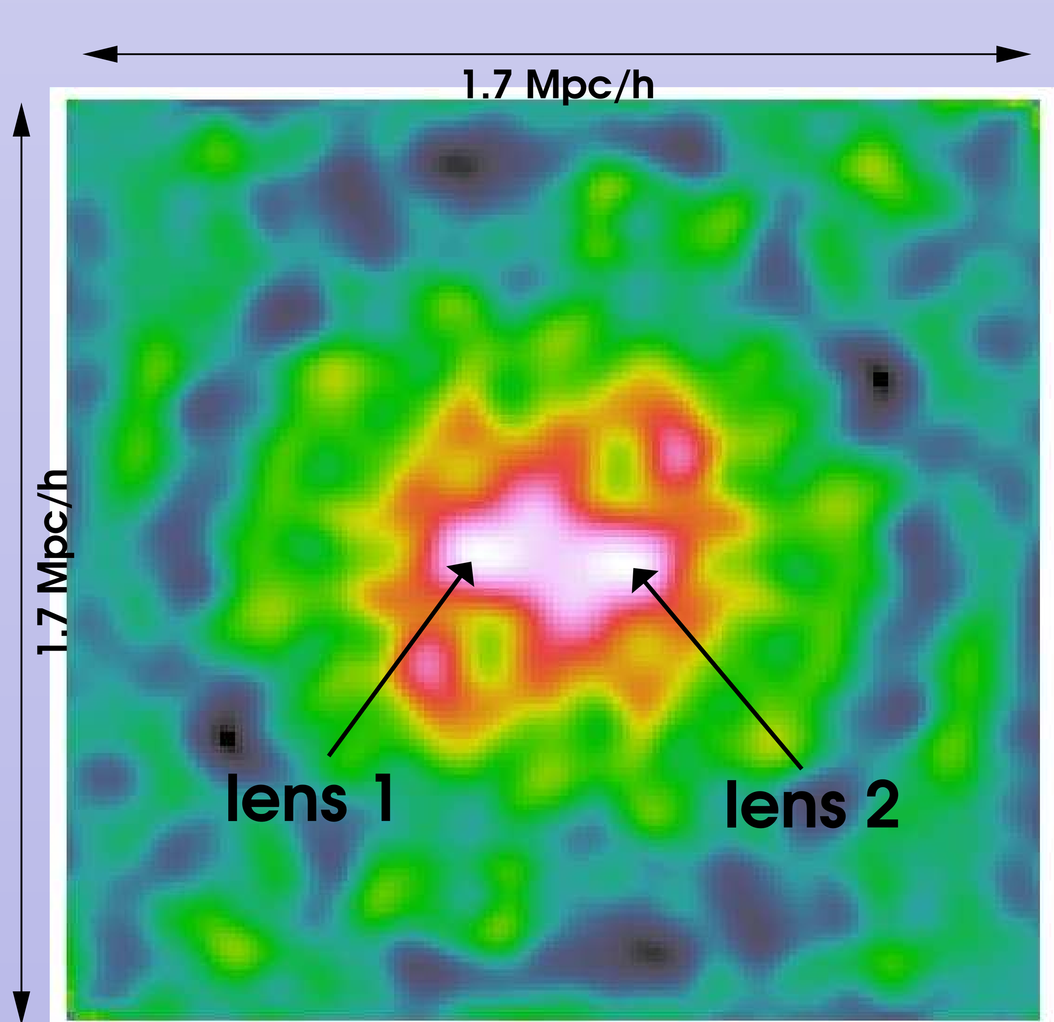

Fig. 3 Possible representation of the lens-lens-shear correlation function as excess matter map about lenses with fixed separation as, e.g., in the Red-Sequence Cluster Survey [2].

Galaxy-galaxy-galaxy lensing (G3L) is a natural extension [1] of galaxy-galaxy lensing (GGL), a frequently employed tool to investigate the typical matter environment about a population of lenses or the correlation of matter and galaxy distribution on a $2^{\rm nd}$-order basis. Contrary to GGL, G3L now involves either two lenses and one source or two sources and one lens, probing the excess matter distribution about two lenses (Fig. 3) and, in the latter case, the lens-to-lens variance of the shear pattern about lenses, see Fig 4 as illustration. It is a three-point correlation function. Here, the G3L correlation functions are transformed into the equivalent $3^{\rm rd}$-order aperture moments statistics [1], either $\langle \mathcal{N}^2 M_{\rm ap} \rangle$ or $\langle \mathcal{N} M_{\rm ap}^2 \rangle$, relating the fluctuations in the lens number density field ($\mathcal{N}$) to those in the lensing convergence field ($M_{\rm ap}$) for a certain filter scale $\theta_{\rm ap}$. They measure the cross-bispectrum between lenses and sources.

References

1. Schneider, P. & Watts, P., 2004, A&A, 2004, 432, 783
2. Simon, P., Watts, P., Schneider, P., Hoekstra, H., et al., 2008, A&A, 479, 655

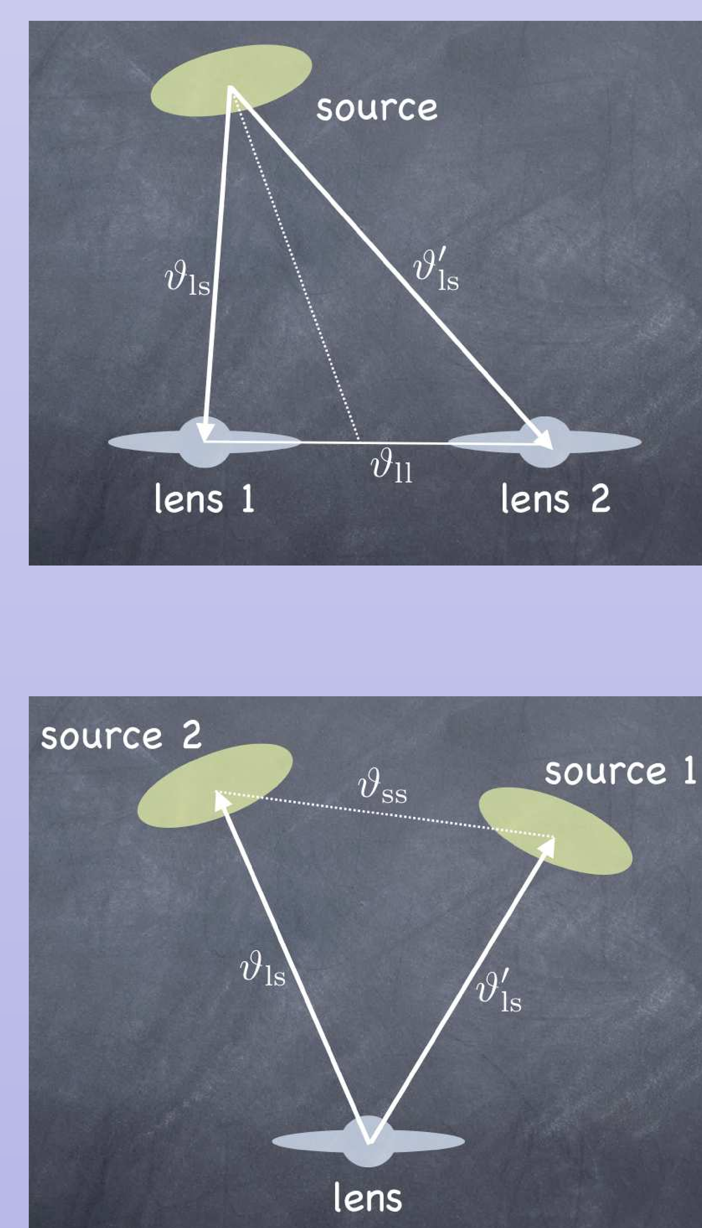

Fig. 4: G3L correlation functions: mean tangential shear about lens pair centres (top) and shear-shear correlation as function of lens separation (bottom). Correlations are measured for a wide range of triangle configurations.